EXHIBIT 4

Mebendazole Elicits a Potent Antitumor Effect on Human Cancer Cell Lines Both *in Vitro* and *in Vivo*[1]

Tapas Mukhopadhyay,[2] Ji-ichiro Sasaki, Rajagopal Ramesh, and Jack A. Roth

Department of Thoracic and Cardiovascular Surgery, The University of Texas M. D. Anderson Cancer Center, Houston, Texas 77030

ABSTRACT

We have found that mebendazole (MZ), a derivative of benzimidazole, induces a dose- and time-dependent apoptotic response in human lung cancer cell lines. In this study, MZ arrested cells at the G_2-M phase before the onset of apoptosis, as detected by using fluorescence-activated cell sorter analysis. MZ treatment also resulted in mitochondrial cytochrome *c* release, followed by apoptotic cell death. Additionally, MZ appeared to be a potent inhibitor of tumor cell growth with little toxicity to normal WI38 and human umbilical vein endothelial cells. When administered p.o. to *nu/nu* mice, MZ strongly inhibited the growth of human tumor xenografts and significantly reduced the number and size of tumors in an experimental model of lung metastasis. In assessing angiogenesis, we found significantly reduced vessel densities in MZ-treated mice compared with those in control mice. These results suggest that MZ is effective in the treatment of cancer and other angiogenesis-dependent diseases.

INTRODUCTION

Microtubules serve as an intracellular scaffold, and their unique polymerization dynamics are critical for many cellular functions (1, 2). It is conceivable that cytoskeletal dysfunction, manifested as either a disrupted microtubule network or stabilized, "rigid" microtubule cytoskeleton, is an intracellular stress. Furthermore, disruption of the equilibrium between tubulin monomers/dimers and microtubule polymers using microtubule-stabilizing (*e.g.*, paclitaxel, docetaxel) or microtubule-destabilizing (*e.g.*, vinblastine, vincristine, nocodazole, colchicine) agents activates the stress-activated protein kinase signaling cascade. Such microtubule disruption is associated with G_2-M-phase blockage (3–7). A number of microtubule drugs have been shown to be highly active, with significant clinical activity against tumor cells. However, most of these drugs are highly toxic, which limits their application. The compounds known as BZs[3] are also known to bind microtubules, but their effect on tumor cells has remained elusive. MZ, a BZ derivative, was first shown to cause mitotic arrest in parasitic cells as early as 1975, and the effects of MZ on mammalian tubulin were published in a series of reports (8–14). We have analyzed both the *in vitro* and *in vivo* effects of MZ on tumor cell growth as well as the molecular mechanisms involved in its action. BZ interacts weakly with host tubulin and affects the microtubule assembly only at high concentrations, whereas MZ is an anthelmintic drug that is used extensively for gastrointestinal parasitic infections in humans. However, the major application of these compounds to date has been the treatment of veterinary and human helminthiasis, in which they have demonstrated remarkable efficacy and safety (15). In this study, we were interested in determining the effect of MZ on solid tumor growth and angiogenesis. Structurally different from other anticancer drugs, MZ is remarkably safe at high doses in humans. We report here evidence indicating that MZ induces G_2-M cell cycle arrest, which ultimately promotes apoptosis in lung cancer cells. Our results demonstrate for the first time the antitumor and antiangiogenetic effects of MZ both *in vitro* and *in vivo*.

MATERIALS AND METHODS

***In Vitro* Cell Culture and Proliferation Assay.** Cells of the human non-small cell lung cancer cell line A549, WI38 normal fibroblasts (American Type Culture Collection, Rockville, MD), and human lung cancer cell lines H1299 and H460 (a gift from Drs. Adi Gazdar and John Minna, The University of Texas Southwestern Medical Center at Dallas, Dallas, TX) were seeded onto culture plates (2×10^4 cells/well) in F12 and RPMI 1640 media, supplemented with 10% heat-inactivated FCS and antibiotics. Also, HUVECs were grown in medium supplemented with growth factor (Clonetics, San Diego, CA). When grown to 40–50% confluence, the cells were exposed to MZ

[3] The abbreviations used are: BZ, benzimidazole; MZ, mebendazole (5-benzoyl-2-benzimidazole carbamatic acid); HUVEC, human umbilical vein endothelial cell; COX IV, cytochrome *c* oxidase subunit IV; IC_{50}, half-maximal inhibitory concentration.

dissolved in DMSO. Cell growth was monitored by counting the viable cells using a hemacytometer.

DNA Fragmentation and Cell Cycle Analysis. Control and MZ-treated cells were washed in cold PBS. The cell pellets were lysed in lysis buffer [10 mM Tris (pH 7.4), 10 mM EDTA (pH 8.0), and 0.5% Triton X-100] and incubated for 10 min at 4°C and then incubated with 200 μg/ml RNase A for 1 h at 37°C. After centrifugation, the supernatants were incubated with 200 μg/ml proteinase K for 30 min at 50°C. Next, DNA fragments were precipitated with 0.5 M NaCl and 50% isopropanol, and the samples were loaded in 2% agarose TBE gel and stained with ethidium bromide.

Growth of Tumor Xenografts in Mice. Before the start of the experiments, mice underwent total-body irradiation (3.5 Gy). One day later, all animals received an injection of 2 × 10^6 H460 tumor cells into the lower right flank. Starting on the day after a 3–5-mm tumor was established, we administered an oral suspension of MZ at the indicated concentration every other day; five mice were used in each group. Similarly, the experiments were repeated in syngeneic C3H mice, and 2 × 10^6 K1735 mouse cells were injected/animal; however, these animals received no radiation. Both control and treated mice were then monitored for tumor growth, with cross-sectional diameter of the tumors measured externally every 7 days. Also, the tumor volume was calculated as described previously (9). The experiments were conducted in triplicate.

Hemoglobin Assay. Quantitation of tumor vascularity was performed by using hemoglobin assay essentially as described previously (16). Briefly, s.c. tumors were excised, weighed, individually frozen in test tubes and, usually 24 h later, thawed. Approximately 20 ml of distilled water/g of tumor tissue were then added, and the tumor was homogenized using a blade homogenizer until it was fully disintegrated. The debris was then pelleted via centrifugation (3000 × g for 5 min), and the supernatant, which contained hemoglobin, was collected. The concentration of hemoglobin in the supernatant was determined according to the catalytic action of hemoglobin on the oxidation of 3,3',5,5'-tetramethylbenzidine by hydrogen peroxide as outlined by the manufacturer (Plasma Hemoglobin kit; Sigma Chemical Co., St. Louis, MO).

Evaluation of Lung Metastases and Treatment *in Vivo*. To establish lung metastases, A549 tumor cells (10^6) were injected into the tail vein of 10 female nude mice as described previously (17). Six days later, we divided the mice into two groups of five each. Group 1 received no treatment, and group 2 received 1 mg of MZ p.o. (100 μg) twice a week for 3 weeks. After 3 weeks, the animals were killed via CO$_2$ inhalation. The mice's lungs were then injected intratracheally with India ink and fixed in Fekete's solution. The therapeutic effect of MZ treatment was determined by counting (without knowledge of which treatment group) the metastatic tumors in each lung under a dissecting microscope. The experiments were performed three times, and data were analyzed and interpreted as being statistically significant if $P < 0.05$, according to the Mann-Whitney test.

Histological Analysis of Blood Vessels in Tumor Xenografts. Five-μm sections of paraffin-embedded tissue samples were stained with H&E and subjected to immunoperoxidase detection of endothelial cells using a CD31 antibody (18).

Vascular areas that stained positively for CD31 (at least five fields/specimen) were analyzed under bright-field microscopy. In all of the staining procedures, we included appropriate negative controls.

Chamber Assay of Angiogenesis. We used the dorsal air sac method (19) to assay angiogenesis *in vivo*. Briefly, 1 × 10^7 cultured A549 cells were suspended in PBS and packed into round cellulose ester membrane chambers having a diameter of 14 mm (pore size, 0.45 μm; Millipore Corp., Bedford, MA). Each chamber was then implanted into a dorsal air sac of a nude mouse. From the next day onward after implantation, the mice were given an oral suspension of MZ (1 mg/mouse/day); five mice were used in each group. The mice were killed on day 5, and the s.c. region overlying the chamber in each mouse was photographed.

Cellular Fractionation for Cytochrome *c* and Western Blot Analysis. We performed cell fractionation using the Apo Alert Cell Fractionation kit (Clontech, Palo Alto, CA) according to the user's manual. In brief, H1299 and H460 cell lines were treated with the indicated dose of MZ for 48 h, washed, and harvested in washing buffer and then homogenized in lysis buffer in an ice-cold Dounce tissue grinder. The cell homogenates were then centrifuged at 700 × g for 10 min at 4°C. Afterward, the supernatants were transferred into 1.5-ml tubes and centrifuged at 10,000 × g for 25 min at 4°C; they were then collected as cytosolic fractions, and the pellets were lysed in lysis buffer and collected as mitochondrial fractions. Western blot analysis was done as described earlier (20). Briefly, the protein concentration in both fractions was determined using the Bradford method (Bio-Rad, Hercules, CA). Next, 25 μg of protein was fractionated using SDS-PAGE, transferred to Amersham membranes (Amersham, Arlington Heights, IL), and immunoblotted with monoclonal antibodies against cytochrome *c*, COX IV, and actin. Immunoreactive proteins were detected using enhanced chemiluminescence (Amersham).

Statistical Analysis. To summarize the study results, we reported descriptive statistics such as the mean and SD. Also, a two-sample Student's *t* test was performed to compare the tumors in control mice with those in mice treated under various conditions.

RESULTS

Effect of MZ on Tumor Cell Growth *in Vitro*. MZ treatment for 48 h strongly inhibited the growth of the lung cancer cell lines (Fig. 1*A*); the IC$_{50}$ was ~0.16 μM. Specifically, MZ induced dose- and time-dependent inhibition of the growth of these cells. However, although MZ was highly cytotoxic to the tumor cells in culture, reducing their number to below the initial plating density, it had no effect on normal HUVECs or WI38 fibroblasts, even at a concentration of 1 μM (Fig. 1*A*). Additionally, we examined the effect of MZ on H460 and A549 human lung cancer cells in a 5-day growth assay (Fig. 1*B*). We found that MZ inhibited growth of the cells 5-fold compared with that of control cells. The growth-inhibitory effect was not restricted to lung cancer cells, because MZ also profoundly inhibited the growth of breast, ovary, and colon carcinomas and osteosarcomas, producing IC$_{50}$s that varied from 0.1 to 0.8 μM (data not shown).

Clinical Cancer Research 2965

Fig. 1 Effect of MZ on cell growth and apoptosis. *A,* dose-dependent inhibition of cell proliferation after MZ treatment. The H460, A549, HU-VEC, and WI38 cell lines were used in this assay. *B,* H460 and A549 cells were treated with 0.165 μM MZ (IC_{50}), and a 5-day growth assay was done. *C,* dose-dependent DNA fragmentation analysis was done in H460 cells after 24 h of MZ treatment. *Lane 1,* controls; *Lanes 2–4,* H460 cells exposed to 0.2, 0.5, and 1.0 μM MZ. *D,* H460 cells treated with MZ, harvested at different time intervals, and stained with propidium iodide. The cells were processed for fluorescence-activated cell sorter analysis to determine the cell cycle phase and apoptosis. Subdiploid populations indicate the apoptotic cells. The phase-contrast photomicrographs (×40) show mitotic cells after 12 h of MZ treatment and apoptotic nuclei after 24 and 48 h of MZ treatment. *Thin arrows,* apoptotic nuclei; *thick arrows,* mitotic nuclei. *E,* cytochrome *c* detected using Western blot analysis in the cytosolic fraction of H1299 and H460 cells. A considerable increase in cytochrome *c* was noticed, which correlated with the MZ dose. An antibody against COX IV, a mitochondria-specific protein, was used to probe the membrane to eliminate the possibility of contamination during fractionation.
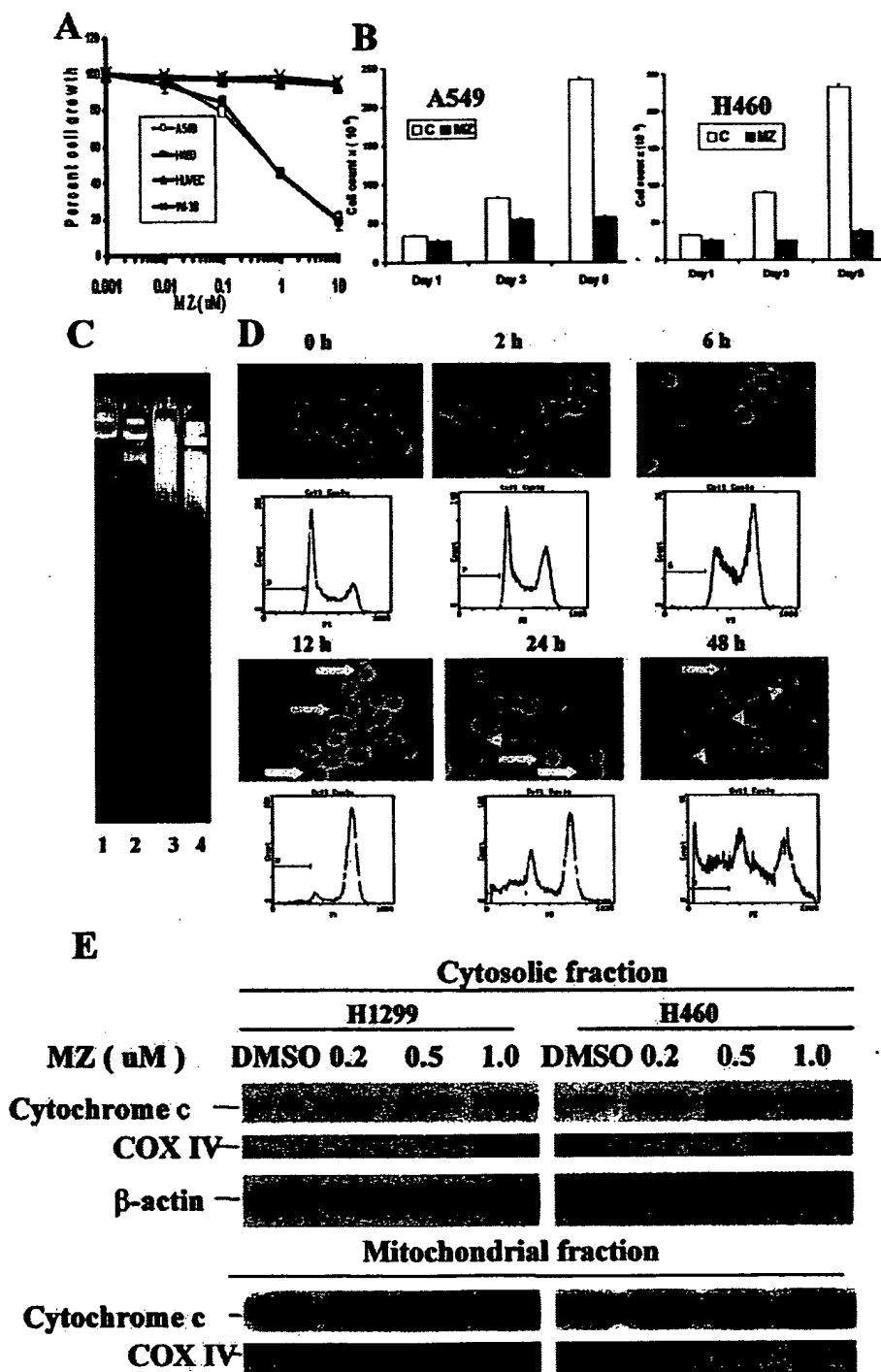
Induction of G_2-M Arrest Followed by Apoptosis by MZ in Lung Cancer Cell Lines.

When cells were treated with various doses of MZ, they were killed as a result of apoptosis. Specifically, H460 cells were exposed to MZ (0.2–5.0 μM for 24 h before the DNA was extracted for agarose gel electrophoresis). Fig. 1C shows that MZ induced DNA fragmentation at 24 h in a dose-dependent manner. The mechanism of cell death was determined to be apoptosis via detection of apoptotic cell populations that displayed a sub-2N genomic content during fluorescence-activated cell sorting (Fig. 1D). We
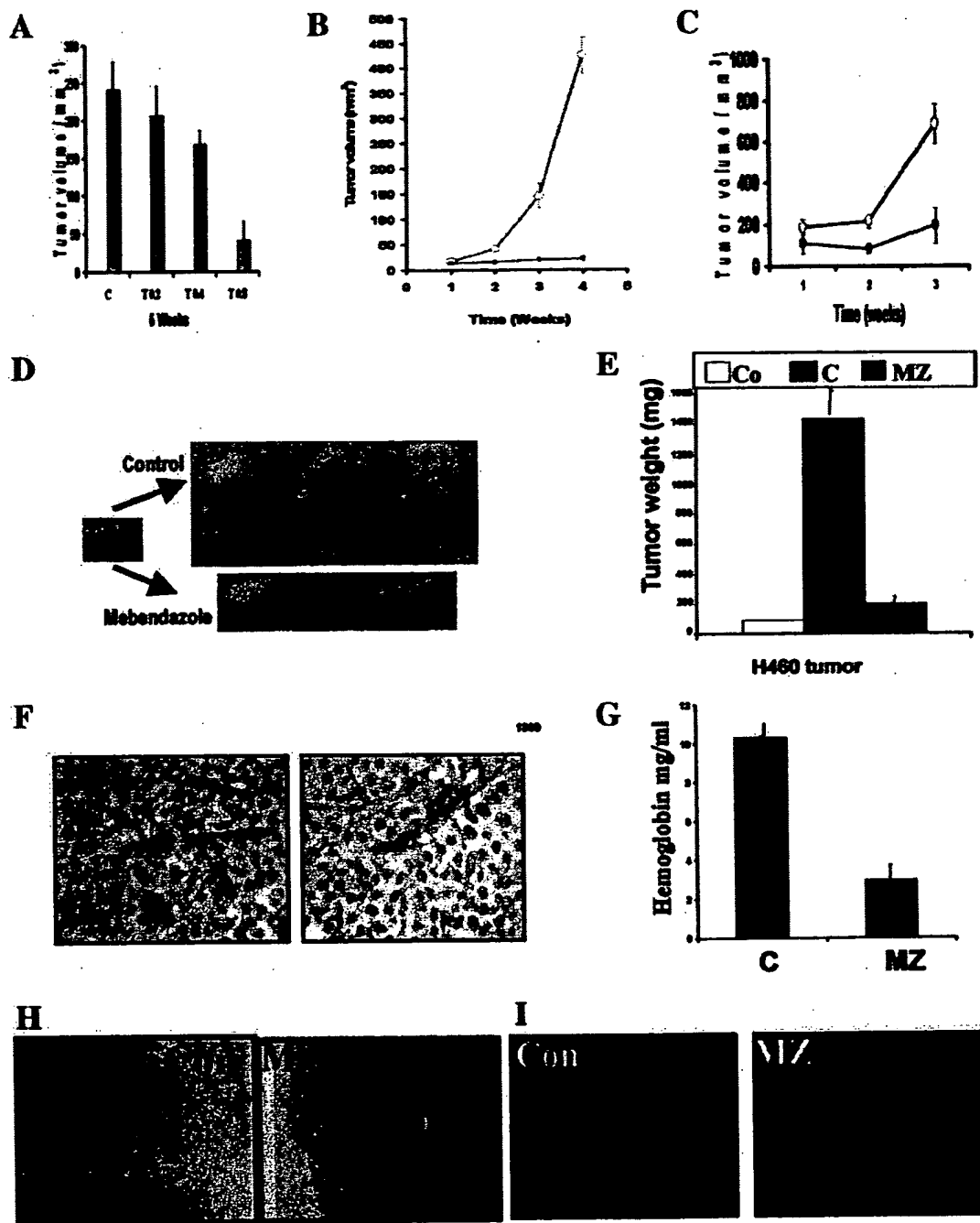
Fig. 2 Effect of MZ on tumor growth and angiogenesis. *A*, MZ inhibited H460 xenograft tumor growth in athymic *nu/nu* mice in a dose-dependent manner. H460 cells were injected into mice (2 × 10^6 cells/mouse), and mice having established tumors (3–4 mm in diameter) were fed different concentrations of MZ (*T02, T04,* and *T08,* 200, 400, and 800 µg of MZ, respectively) every other day, whereas control animals received PBS. *B*, significant growth inhibition was observed when *nu/nu* mice were fed 1 mg of MZ every other day. O, control mice; ●, MZ-treated mice. *Bars,* SE. *C,* as expected, K1735 mouse xenografts in C3H mice showed reduced tumor growth when the mice were fed with 1 mg of MZ every other day. *D,* tumors were excised from control and MZ-treated *nu/nu* mice after 4 weeks and photographed. A few mice were killed at the start of treatment, when the tumors had reached 3–4 mm in diameter. *E,* graphic representation of the weight (mg ± SD) of tumors in control. Co, approximate tumor weight of ~3–5 mm diameter tumor before starting MZ treatment; *C,* untreated and MZ-treated mice on day 28. *F,* histological analysis of blood vessels in H460 xenograft tumors via immunoperoxidase detection of endothelial cells using a CD31 antibody. *I,* control untreated; *2,* MZ treated. *G,* plot of milligrams of hemoglobin/ml of tumor tissue obtained from control and treated animals after hemoglobin assay. *C,* control; *MZ,* treated. *H,* effect of MZ on angiogenesis *in vivo.* Chamber assay shows that MZ inhibited capillary formation in A549 cells. It should be noted that the control implant had a tree-like architecture of major vessels (*arrow*) connecting to minor branches but that the MZ-treated implants had scarce vessels. *Con,* control; *MZ,* treated. *I,* A549 cells prelabeled using a fluorescent cell marker were detected on the chamber membranes of control (*Con*) and MZ-treated (*MZ*) mice.

found that the cells were blocked at the G_2-M phase 12 h after MZ treatment before undergoing apoptosis. Cells were rounded and partly detached after 12 h of MZ treatment. However, after 24 h of treatment, cell shrinkage occurred, and nuclear bodies were evident; the cells subsequently underwent apoptosis. After 48 h of MZ treatment, >60% of the cells had undergone apoptosis with characteristic nuclear fragmentation (Fig. 1D). In addition, a number of apoptotic gene family proteins were examined using Western blot analysis. It was found that p53 protein is posttranslationally stabilized and elevated without an increase in mRNA (data not shown). This occurs so frequently during apoptosis induced by diverse stress stimuli that it has been considered a common feature of the p53-induced apoptotic process (21). Furthermore, as a consequence of p53 stabilization, expression of the p53 target genes p21 and MDM2 was also induced. However, MZ had no effect on protein expression of genes belonging to the Bcl2 family, including Bcl-xl, bax, bad, and bak, as determined via Western blot analysis (data not shown).

Induction of Cytochrome c Release and Caspase Activation by MZ. Because MZ could inhibit the growth of p53-null cell lines and other p53-mutated cells, although at a higher dose, we examined the other p53-independent pathways. To examine whether MZ signaling goes through a mitochondrial pathway, H1299 (p53-null) and H460 (p53 wild-type) cells were treated with MZ in a dose-dependent manner, and cytosolic extracts lacking mitochondria were prepared and analyzed via immunoblotting (Fig. 1E). Cytochrome c accumulated in cytosolic extracts at 12 h after exposure to MZ increased in both of the cell lines in a dose-dependent manner. Also, the membranes were probed using an antibody against COX IV, a protein that is specific for mitochondria, as an internal control. Both cell lines showed an increase in cytochrome c protein in the cytoplasm after MZ treatment in a dose-dependent manner. Twenty-four h after MZ treatment, activation of caspase-9 and caspase-8 and cleavage of the caspase substrate poly(ADP-ribose) polymerase and procaspase-3 were detectable (data not shown).

Inhibition of Tumor Cell Growth and Angiogenesis by MZ. The effect of MZ on the proliferation of tumor cell lines in vitro prompted us to investigate its antitumor activity in a nu/nu mouse model. We established tumors in the mice by s.c. injecting them with 1×10^6 H460 cells, which are human non-small cell lung cancer cells. A dose-escalation study indicated that MZ suppressed growth of the tumors in a dose-dependent manner (Fig. 2A). Specifically, mice having established tumors (~3 mm in diameter) were fed 1 mg of MZ p.o. every other day, which was sufficient to profoundly inhibit tumor growth (Fig. 2B). The experiment was repeated with C3H mice and the K1735 mouse cell line, and MZ showed inhibited tumor growth in a syngeneic mouse model (Fig. 2C). H460 tumors were then harvested, photographed (Fig. 2D), and weighed. The experiment was repeated twice using 10 animals in both the control and treatment groups. We found a marked difference in tumor weight between the MZ-treated and control animals (Fig. 2E). Additionally, in control mice, the xenograft of H460 cells exhibited a marked increase in tumor growth kinetics compared with that in mice in the MZ-treated group. Furthermore, MZ-treated mice showed no signs of toxicity and

were all healthier than the control mice were during the 4 weeks of treatment (data not shown).

To determine whether the differences in growth kinetics observed in vivo were associated with variations in tumor vascularity, sections of s.c. tumors established from H460 cells were stained for CD31, a marker expressed by endothelial cells. A significant decrease in the number of CD31-positive endothelial cells was observed in MZ-treated mice when compared with that in control mice. This analysis demonstrated substantially increased blood vessel density in untreated mice compared with that in MZ-treated mice (Fig. 2F). Thus, MZ treatment profoundly reduced the neovascularization and growth of human lung cancer xenografts in nude mice. This tumor-suppressing effect of MZ may have been attributable to inhibition of tumor-induced angiogenesis. In addition, the tumor vascularity in vivo was quantitated in control and MZ-treated mice using a hemoglobin assay. The results of this assay indicated that there was a 75% reduction in hemoglobin content/gram of tumor sample obtained from MZ-treated mice, as compared with control mice (Fig. 2G).

Angiogenesis in vivo was further assayed using the dorsal air sac method (22) by photographing the area of s.c. neovascularization in mice overlying a semipermeable membrane chamber containing H460 or A549 cells. Twenty-four h after each chamber was implanted, the animals were fed 1 mg of MZ p.o. every other day for a total of three treatments. Both the number and caliber of the blood vessels were significantly reduced in mice treated with MZ compared with those in control mice (Fig. 2H). To exclude the possibility that the reduced vasculature was attributable to a lack of viable tumor cells in the chamber, we prelabeled tumor cells using a fluorescent dye before injecting them into the chamber. After photographing the blood vessels, we examined the tumor cells on the membrane using a fluorescence microscope. The results indicated that the control and MZ-treated mice had similar cell densities on the membrane filters (Fig. 2I).

Next, we sought to determine whether MZ treatment would inhibit the growth of human lung cancer colony formation in an experimental lung metastasis model. In this study, ~300 metastatic colonies appeared in the lungs of control mice 21 days after the injection of A549 cells via the tail vein (Figs. 3, A and B). However, the oral administration of 1 mg of MZ/mouse every other day reduced the mean colony count to 80% of the mean count in control mice ($P < 0.0001$). This experiment was performed three times with similar results. In a control experiment, mice that were treated using paclitaxel alone did not show a significant reduction in colony formation (data not shown). Histochemical staining of lung tissues using H&E indicated that not only the number but also the size of the metastatic tumor colonies (as measured according to the transverse diameter of the tumor colony) was substantially reduced by treatment using MZ (Fig. 3C). A number of cells with fragmented nuclei were detectable in the histological section.

DISCUSSION

MZ is one of the truly broad-spectrum anthelmintics, the BZs, which have a high therapeutic index. Central to the success of the BZs is their selective toxicity in helminths. Although the
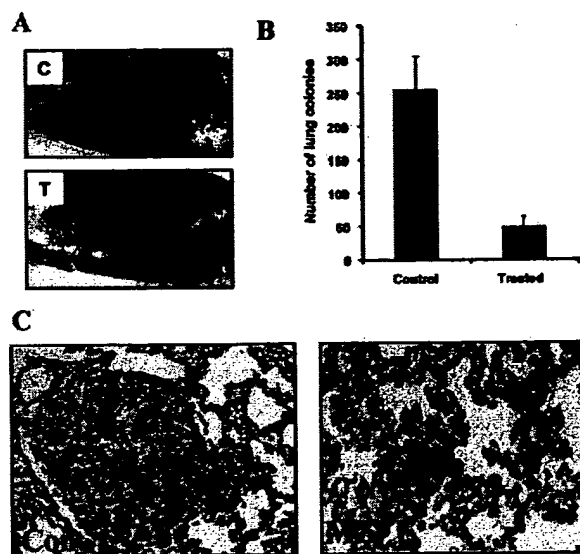
A   **B**

C

Fig. 3 Effect of MZ treatment on lung colony formation in an experimental metastasis. *A*, A549 cells formed colonies on lung surfaces when injected through the tail vein. *C*, control mouse received no treatment; *T*, MZ-treated mice received 1 mg of MZ p.o. twice a week for 3 weeks. The *white spots* on the lung surfaces (*arrows*) are colonies. *B*, quantitation of lung colonies in control and MZ-treated animals ($P <$ 0.0001); the total number of lung colonies/animal were plotted. *C*, H&E-stained lung sections show the sizes of tumor colonies in control (*Con*) and MZ-treated (*MZ*) animals. The colonies are indicated by *dotted lines*.

diverse activities of these compounds have been described at both the biochemical and cellular levels, their molecular mechanism of action has not been explored in detail; when it has been studied, this mechanism has proven to be controversial. BZs are known to act via a wide variety of apparently unrelated mechanisms. Of these mechanisms, fumarate reductase, glucose uptake, and microtubule inhibition satisfy many of the criteria considered relevant for a putative site of action. This gives rise to the question of whether these mechanisms are directly or indirectly related. On the basis of the inhibitor profile of both fumarate reductase and glucose uptake, it is apparent that these systems are not specific to BZs, and thus most studies support the hypothesis of microtubule dependence of the action of BZs.

However, data exist that support a general concept of primary microtubule action leading to a series of biochemical effects that either directly or indirectly elicit a number of changes; as we demonstrate here, these changes vary in normal and cancer cells. The results of binding studies using enriched extracts from the tubulin of helminths and mammals have suggested BZs as mictotubule depolymerizing agents (15, 23, 24). However, the results of crystallographic and other studies have indicated that the tubulin-binding site of BZs is distinctly different from that of other microtubule-disrupting agents such as vinblastine and paclitaxel. Drugs in the latter group bind to tubulin at sites located near the intradimer interface and facing the lumen of the microtubule, whereas the possible binding site for BZs is on the outside of the microtubule (25, 26). Although

BZs are known as microtubule poisons, a comparison of their relative activity showed that some structural refinement produces BZ derivatives, such as MZ, that are significantly less active against mammalian tubulin. Also, BZs have been reported to have poor systemic absorption after oral administration *in vivo*. The observed safety of the BZs as anthelmintics may also be unrelated to BZ-tubulin binding but rather may be attributable to differences in the metabolic or detoxification pathways as suggested by Nare *et al.* (27). For example, rapid, extensive metabolism of BZs into less toxic metabolites (*e.g.,* sulfoxides and sulfones) by the hepatic microsomal enzymes (28, 29) may account for some of the lack of host toxicity. Parasites, on the other hand, lack these metabolic pathways and are killed by BZs. Additionally, some terbenzimidazole compounds have been reported to be topoisomerase I poisons (30); therefore, we tested MZ for such an effect but could not detect it.[4]

The effect of MZ as an antitumor agent has never been tested before. With that in mind, one of our most encouraging findings was that MZ inhibited neovascularization both *in vitro* and in the human xenografts we tested, indicating that MZ is a potent antiangiogenic agent. Although the reduced vascularity in MZ-treated tumors was evident from the CD31 staining, future studies are needed to compare the vessel density between control and MZ-treated tumors of the same size. This will allow us to conclude whether MZ-induced tumor growth inhibition is attributable to inhibition of nasovascularization or is a consequence of reduced tumor cell growth. In our dorsal air sac study, when sacs containing the tumor cells were further stained with Hoechst 33258 and observed under a fluorescence microscope, a significant number of cells showed apoptotic nuclei and DNA fragmentation (data not shown), which supports our *in vitro* data and may contribute to reduced vessel formation. Moreover, MZ had no effect on normal endothelial cell growth but directly targeted tumor cells *in vivo*. Although the molecular mechanism of the action of MZ on tumor growth inhibition requires further elucidation, our results show that MZ may be effective in the treatment of cancer and other angiogenesis-dependent diseases.

ACKNOWLEDGMENTS

REFERENCES

1. McNally, F. J. Modulation of microtubule dynamics during the cell cycle. Curr. Opin. Cell Biol., *8:* 23–29, 1996.

2. Saunders, C., and Limbird, L. E. Disruption of microtubules reveals two independent apical targeting mechanisms for G-protein-coupled receptors in polarized renal epithelial cells. J. Biol. Chem., *272:* 19035–19045, 1997.

3. Manfredi, J. J., and Horwitz, S. B. Taxol: an antimitotic agent with a new mechanism of action. Pharmacol. Ther., *25:* 83–125, 1984.

4. Rowinsky, E. K., and Donehower, R. C. Paclitaxel (Taxol). N. Engl. J. Med., *332:* 1004–1014, 1995.

5. Bhalla, K., Ibrado, A. M., Tourkina, E., Tang, C., Mahoney, M. E., and Huang, Y. Taxol induces internucleosomal DNA fragmentation

_____

[4] Unpublished results.

associated with programmed cell death in human myeloid leukemia cells. Leukemia (Baltimore), 7: 563–568, 1993.

6. Long, B. H., and Fairchild, C. R. Paclitaxel inhibits progression of mitotic cells to G1 phase by interference with spindle formation without affecting other microtubule functions during anaphase and telephase. Cancer Res., 54: 4355–4361, 1994.

7. Horwitz, S. B. Mechanism of action of Taxol. Trends Pharmacol. Sci., 13: 134–136, 1992.

8. Delatour, P., and Richard, Y. Embryotoxic and antimitotic properties of some benzimidazole related compounds. Therapie, 31: 505–515, 1976.

9. Friedman, P. A., and Platzer, E. G. Interaction of anthelmintic benzimidazoles and benzimidazole derivatives with bovine brain tubulin. Biochim. Biophys. Acta, 544: 605–614, 1978.

10. Ireland, C. M., Gull, K., Gutteridge, W. E., and Pogson, C. I. The interaction of benzimidazole carbamates with mammalian microtubule protein. Biochem. Pharmacol., 28: 2680–2682, 1979.

11. Laclette, J. P., Guerra, G., and Zetina, C. Inhibition of tubulin polymerization by mebendazole. Biochem. Biophys. Res. Commun., 92: 417–423, 1980.

12. Kohler, P., and Bachmann, R. Intestinal tubulin as possible target for the chemotherapeutic action of mebendazole in parasitic nematodes. Mol. Biochem. Parasitol., 4: 325–336, 1981.

13. Lacey, E., and Watson, T. R. Structure-activity relationships of benzimidazole carbamates as inhibitors of mammalian tubulin, in vitro. Biochem. Pharmacol., 34: 1073–1077, 1999.

14. Russell, G. J., Gill, J. H., and Lacey, E. Binding of [³H]benzimidazole carbamates to mammalian brain tubulin and the mechanism of selective toxicity of the benzimidazole anthelmintics. Biochem. Pharmacol., 43: 1095–1100, 1992.

15. Lacey, E. The role of the cytoskeletal protein, tubulin, in the mode of action and mechanism of drug resistance to benzimidazoles. Int. J. Parasitol., 18: 885–936, 1988.

16. Parish, C. R., Freeman, C., Brown, K. J., Francis, D. J., and Cowden, W. B. Identification of sulfated oligosaccharide-based inhibitors of tumor growth and metastasis using novel in vitro assays for angiogenesis and heparanase activity. Cancer Res., 59: 3433–3441, 1999.

17. Kataoka, M., Schumacher, G., Cristiano, R. J., Atkinson, E. N., Roth, J. A., and Mukhopadhyay, T. An agent that increases tumor suppressor transgene product coupled with systemic transgene delivery inhibits growth of metastatic lung cancer in vivo. Cancer Res., 58: 4761–4765, 1998.

18. Schumacher, G., Kataoka, M., Roth, J. A., and Mukhopadhyay, T. Potent antitumor activity of 2-methoxyestradiol in human pancreatic cancer cell lines. Clin. Cancer Res., 5: 493–499, 1999.

19. Bouvet, M., Ellis, L. M., Nishizaki, M., Fujiwara, T., Liu, W., Bucana, C. D., Fang, B., Lee, J. J., and Roth, J. A. Adenovirus-mediated wild-type p53 gene transfer downregulates vascular endothelial growth factor expression and inhibits angiogenesis in human colon cancer. Cancer Res., 58: 2288–2292, 1998.

20. Nakamura, S., Roth, J. A., and Mukhopadhyay, T. Multiple lysine mutations in the C-terminal domain of p53 interfere with MDM2-dependent protein degradation and ubiquitination. Mol. Cell. Biol., 20: 9391–9398, 2000.

21. Chen, X., Ko, L. J., Jayaraman, L., and Prives, C. p53 levels, functional domains, and DNA damage determine the extent of the apoptotic response of tumor cells. Genes Dev., 10: 2438–2451, 1996.

22. Tanaka, N. G., Sakamoto, N., Inoue, K., Korenaga, H., Kadoya, S., Ogawa, H., and Osada, Y. Antitumor effects of an antiangiogenic polysaccharide from an Arthrobacter species with or without a steroid. Cancer Res., 49: 6727–6730, 1989.

23. Lubega, G. W., and Prichard, R. K. Specific interaction of benzimidazole anthelmintics with tubulin from developing stages of thiabendazole-susceptible and -resistant Haemonchus contortus. Biochem. Pharmacol., 41: 93–101, 1991.

24. Lacey, E., and Prichard, R. K. Interactions of benzimidazoles (BZ) with tubulin from BZ-sensitive and BZ-resistant isolates of Haemonchus contortus. Mol. Biochem. Parasitol., 19: 171–181, 1986.

25. Hamel, E. Antimitotic natural products and their interactions with tubulin. Med. Res. Rev., 16: 207–231, 1996.

26. Downing, K. H. Structural basis for the interaction of tubulin with proteins and drugs that affect microtubule dynamics. Annu. Rev. Cell Dev. Biol., 16: 89–111, 2000.

27. Nare, B., Lubega, G., Prichard, R. K., and Georges, E. p-Azidosalicyl-5-amino-6-phenoxybenzimidazole photolabels the N-terminal 63–103 amino acids of Haemonchus contortus β-tubulin 1. J. Biol. Chem., 271: 8575–8581, 1996.

28. Lanusse, C. E., Nare, B., Gascon, L. H., and Prichard, R. K. Metabolism of albendazole and albendazole sulphoxide by ruminal and intestinal fluids of sheep and cattle. Xenobiotica, 22: 419–426, 1992.

29. Lanusse, C. E., Nare, B., and Prichard, R. K. Comparative sulphoxidation of albendazole by sheep and cattle liver microsomes and the inhibitory effect of methimazole. Xenobiotica, 23: 285–295, 1993.

30. Pilch, D. S., Xu, Z., Sun, Q., Lavoie, E. J., Liu, L. F., Geacintov, N. E., and Breslauer, K. J. Characterizing the DNA binding modes of a topoisomerase I-poisoning terbenzimidazole: evidence for both intercalative and minor groove binding properties. Drug Design Discovery, 13: 115–133, 1996.